Supporting Information for "On the ridging of the South Atlantic Anticyclone over South Africa: the impact of Rossby wave breaking and of climate change"

Ioana Ivanciu[1], Thando Ndarana[2], Katja Matthes[1]and Sebastian Wahl[1]

[1]GEOMAR Helmholtz Centre for Ocean Research Kiel, Germany

[2]Department of Geography, Geoinformatics and Meteorology, University of Pretoria, South Africa

Contents of this file

1. Text S1, S2 and S3
2. Figures S1, S2, S3, S4, S5, S6 and S7

Introduction The supporting material provides detailed descriptions of the algorithms used to identify ridging highs and Rossby wave breaking (RWB) in the South African sector. Additionally, composites of ridging highs with and without Rossby wave breaking based on the ERA5 reanalysis are provided for comparison and validation of the results

---

Corresponding author: I. Ivanciu, GEOMAR Helmholtz Centre for Ocean Research Kiel, Düsternbrooker Weg 20, 24105 Kiel, Germany. (iivanciu@geomar.de)

based on the coupled climate model FOCI. Finally, seasonal composites of precipitation and 850 hPa winds for ridging highs with and without RWB are provided.

S1. Ridging Highs Identification

We identify the ridging of the South Atlantic Anticyclone over South Africa based on MSLP using the method of (Ndarana et al., 2018). For each day, contours are generated, in 1 hPa intervals, from the minimum to the maximum MSLP in the domain 0°- 60°S and 60°W - 60°E. Only closed contours originating in the South Atlantic Ocean and having a diameter of at least 10° are kept, in order to exclude sub-synoptic-scale processes and to ensure that we only consider the South Atlantic Anticyclone and not other high pressure systems. The eastward extension of the contours is then checked starting from the contour with the lowest MSLP and, if a contour extends eastward of 25°E, a ridging event is considered to have occurred. This contour is then saved together with all the contours concentric with it, for that respective day. Since a ridging event can last more than a day, consecutive days with contours extending past 25°E are considered to be part of the same event.

S2. Rossby Wave Breaking Identification

RWB events that are relevant for the South Atlantic Anticyclone are identified using potential vorticity (PV) between -2.5 PVU to -1.5 PVU (1 PVU = $10^6\ K\ m^2\ s^{-1}\ kg^{-1}$) on the 330, 340 and 350 K isentropic surfaces. We follow the algorithm proposed by Ndarana and Waugh (2011) with the additional condition that PV contours need to have an S-like shape, as detailed below.

First, we compute PV on pressure levels:

$$PV = g\Big[f + \frac{1}{acos\phi}\frac{\partial v}{\partial \lambda} - \frac{1}{acos\phi}\frac{\partial (ucos\phi)}{\partial \phi}\Big]\Big(-\frac{\partial \theta}{\partial p}\Big) \quad (1)$$

where g is the gravitational acceleration, f is the Coriolis parameter, a is the radius of the earth, u and v are the zonal and meridional velocity components, respectively, θ is the potential temperature, p is the pressure and ϕ and λ are the latitude and longitude, respectively. Then we linearly interpolate the PV to isentropic surfaces following Edouard, Vautard, and Brunet (1997) and we apply a spatial 3-point running mean. PV contours are generated every 0.1 PVU for each day and isentropic surface. Only contours that are equal to a latitude circle or longer are included in order to exclude isolated PV anomalies that are likely to be remnants of old RWB events. RWB occurs when all the following conditions are met: a meridian intersects a contour at least at three distinct latitudes, the meridional PV gradient is negative and the contour has an S-like shape in the respective region. Additionally, the contour segment has to be at least 20° long. If these conditions are met at the same location for several contours, on several isentropic surfaces or for consecutive day, a single event is considered to have occurred.

S3. Composite Analysis

We perform a composite analysis to identify differences between ridging highs that occur with and without RWB. First, anomalies with respect to the time mean, 1980-2009 for the past and 2070-2099 for the future, are computed. Where seasonal composites are shown, the anomalies are computed with respect to the seasonal mean. Then, composites are taken for each individual member of an ensemble. Finally, the composites for one

ensemble are averaged over its members. The statistical significance of the composites is assessed using the Monte Carlo method.

References

Edouard, S., Vautard, R., & Brunet, G. (1997). On the maintenance of potential vorticity in isentropic coordinates. *Quarterly Journal of the Royal Meteorological Society*, *123*(543), 2069-2094. doi: 10.1002/qj.49712354314

Ndarana, T., Bopape, M.-J., Waugh, D., & Dyson, L. (2018). The Influence of the Lower Stratosphere on Ridging Atlantic Ocean Anticyclones over South Africa. *Journal of Climate*, *31*(15), 6175 - 6187. doi: 10.1175/JCLI-D-17-0832.1

Ndarana, T., & Waugh, D. W. (2011). A Climatology of Rossby Wave Breaking on the Southern Hemisphere Tropopause. *Journal of the Atmospheric Sciences*, *68*(4), 798 - 811. doi: 10.1175/2010JAS3460.1

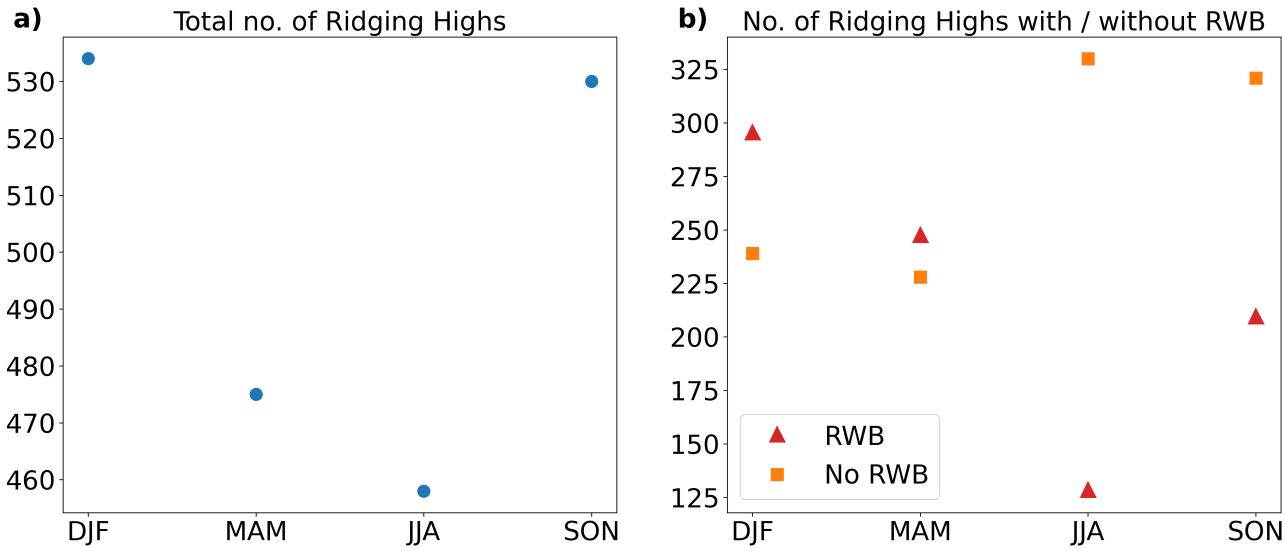

Figure S1. Seasonal distribution of ridging highs in ERA5 for the period 1980-2009: total number of events (a) and number of events with RWB (red triangles) and without RWB (orange squares) (b).

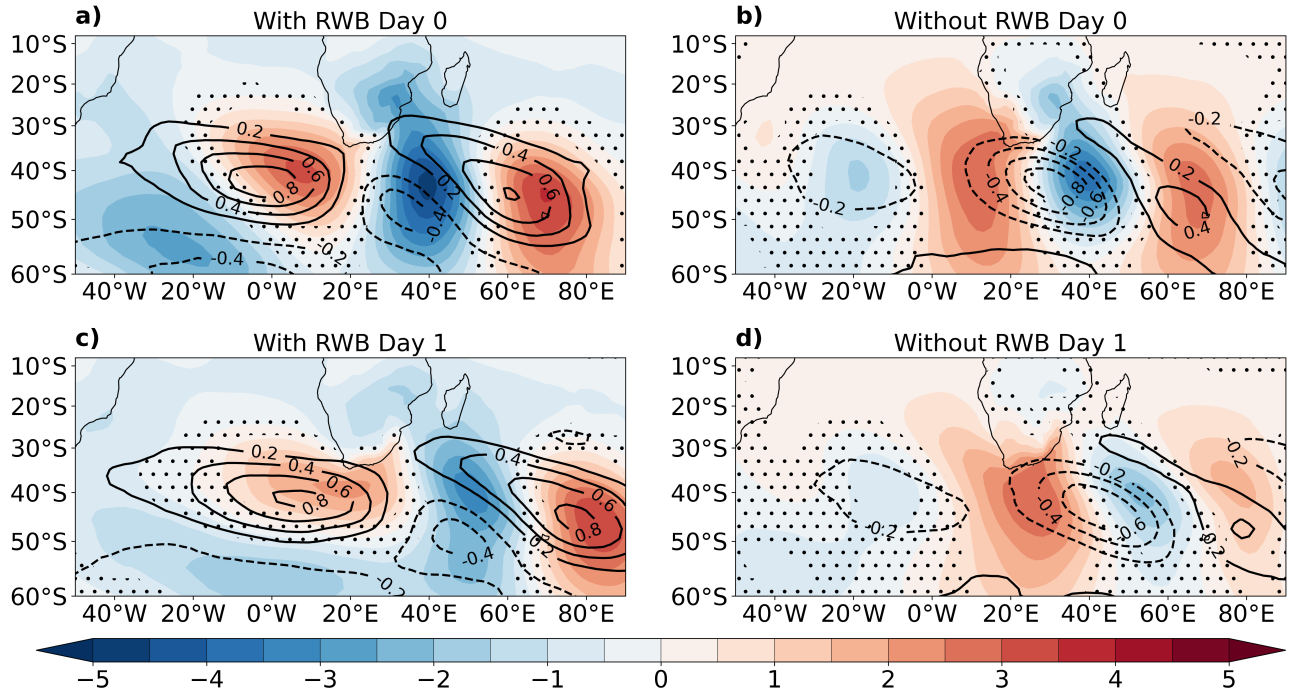

Figure S2. ERA5 composites of ridging highs with (a,c) and without (b,d) RWB at day 0 (a,b) and day 1 (c,d) of the ridging for the period 1980-2009. Anomalies of MSLP (hPa) and of 200 hPa PV (PVU) are depicted by the color shading and by the contours, respectively. The stippling masks anomalies that are **not** significant at the 95% confidence interval based on the Monte Carlo method. Only significant PV anomalies are plotted.

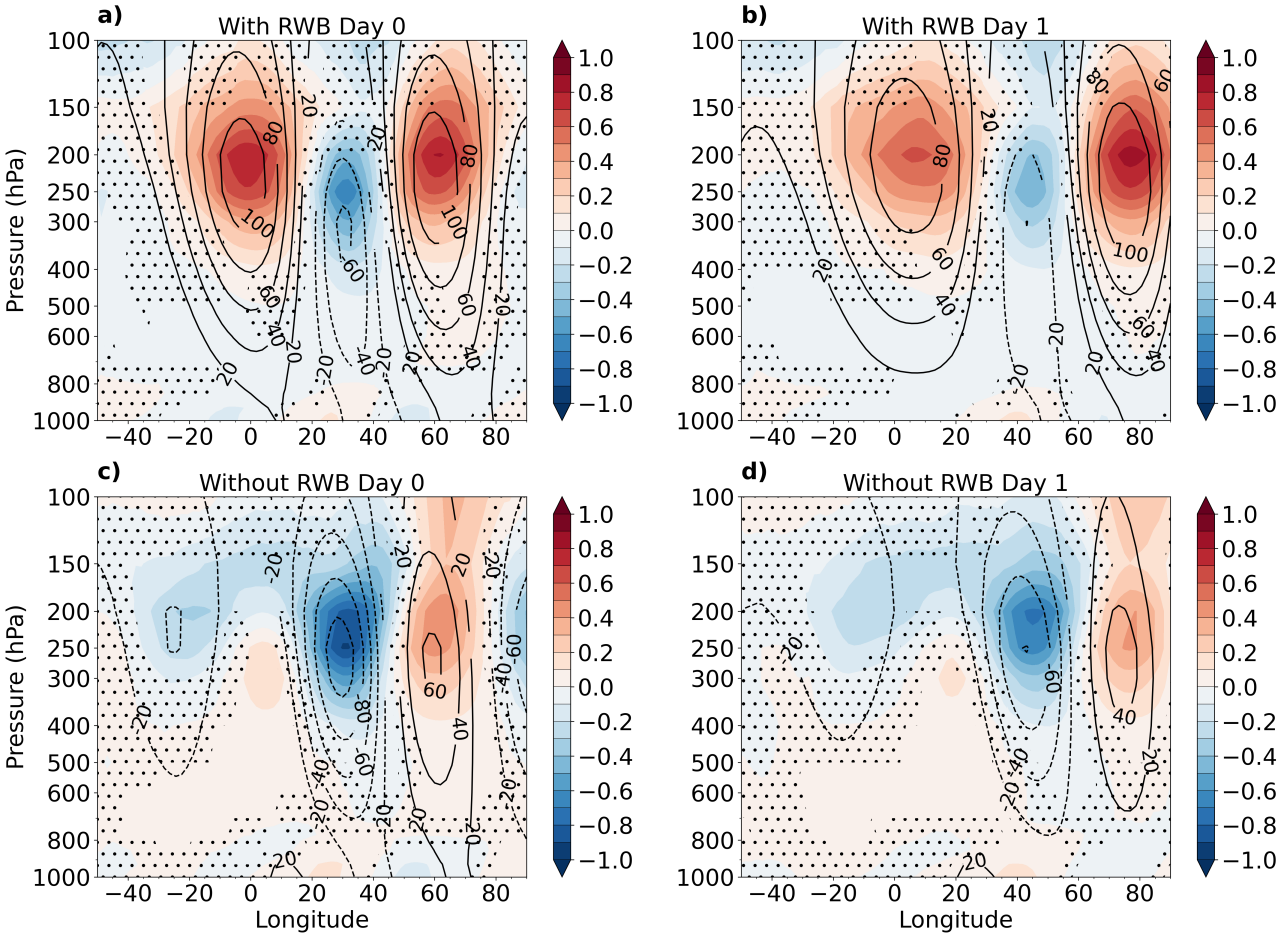

Figure S3. ERA5 composites of ridging highs with (a,b) and without (c,d) RWB at day 0 (a,c) and day 1 (b,d) for the period 1980-2009. Anomalies of PV (PVU) and of geopotential height (m) at 45°S are depicted by the color shading and by the contours, respectively. The stippling masks anomalies that are **not** significant at the 95% confidence interval based on the Monte Carlo method. Only significant geopotential height anomalies are plotted.

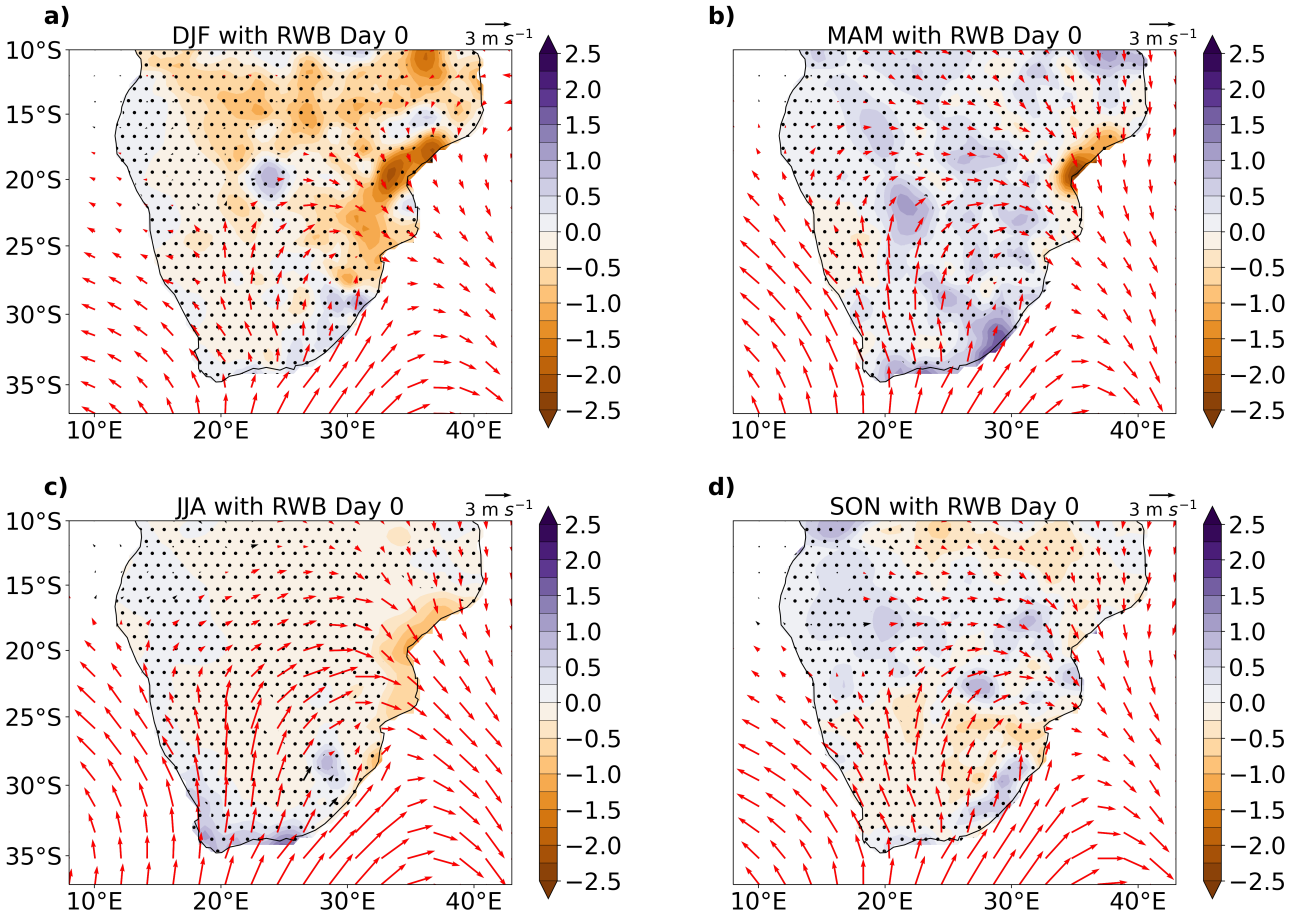

Figure S4. Seasonal composites of day 0 of ridging highs with RWB from observations for the period 1980-2009 for summer (a), autumn (b), winter (c) and spring (d). Seasonal anomalies of precipitation (mm day^{-1}) are depicted by the color shading and seasonal anomalies of the 850 hPa winds (m s^{-1}) are depicted by the vectors. The stippling masks anomalies that are **not** significant at the 95% confidence interval based on the Monte Carlo method. The red vectors depict significant wind anomalies.

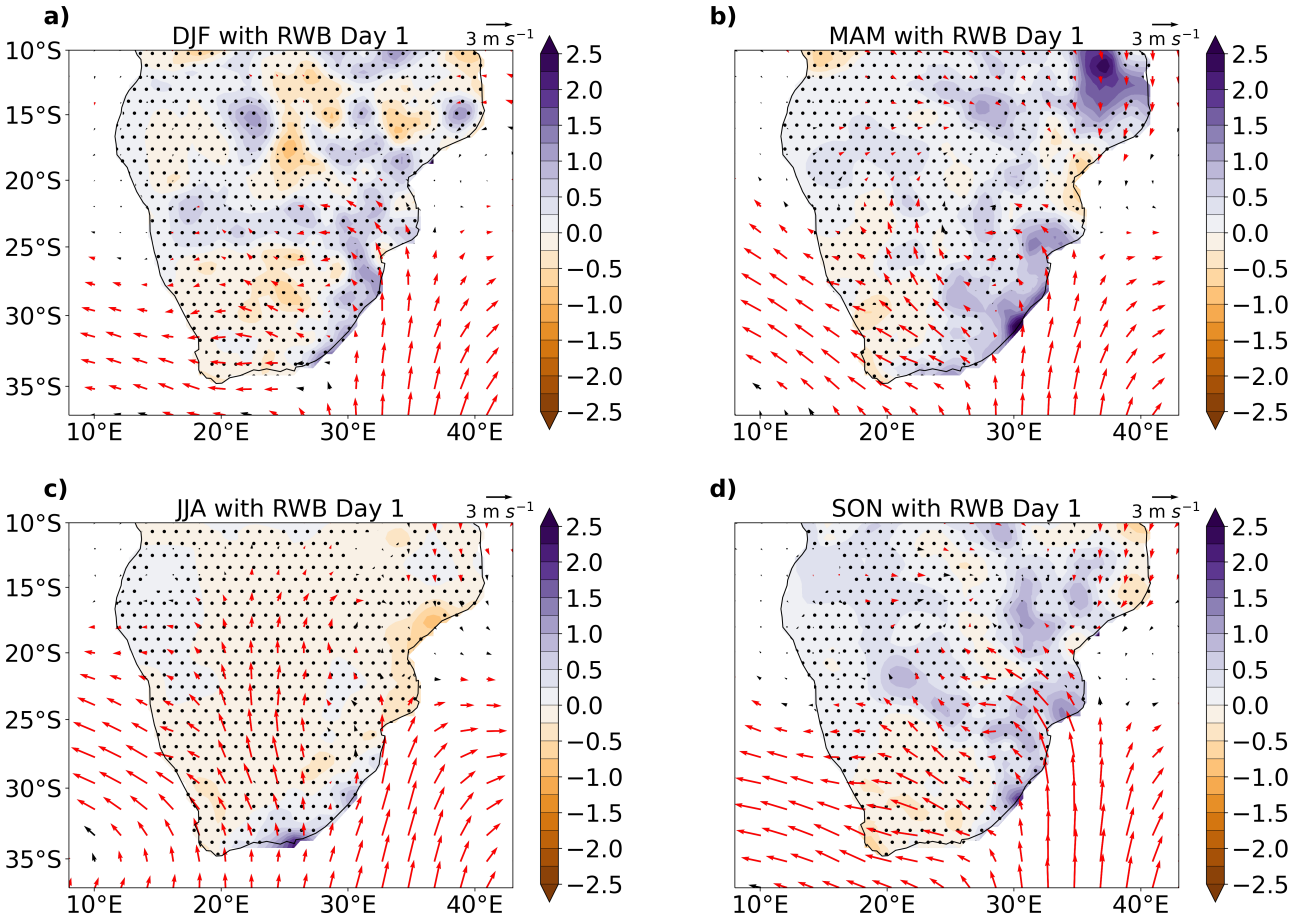

Figure S5. Seasonal composites of day 1 of ridging highs with RWB from observations for the period 1980-2009 for summer (a), autumn (b), winter (c) and spring (d). Seasonal anomalies of precipitation (mm day^{-1}) are depicted by the color shading and seasonal anomalies of the 850 hPa winds (m s^{-1}) are depicted by the vectors. The stippling masks anomalies that are **not** significant at the 95% confidence interval based on the Monte Carlo method. The red vectors depict significant wind anomalies.

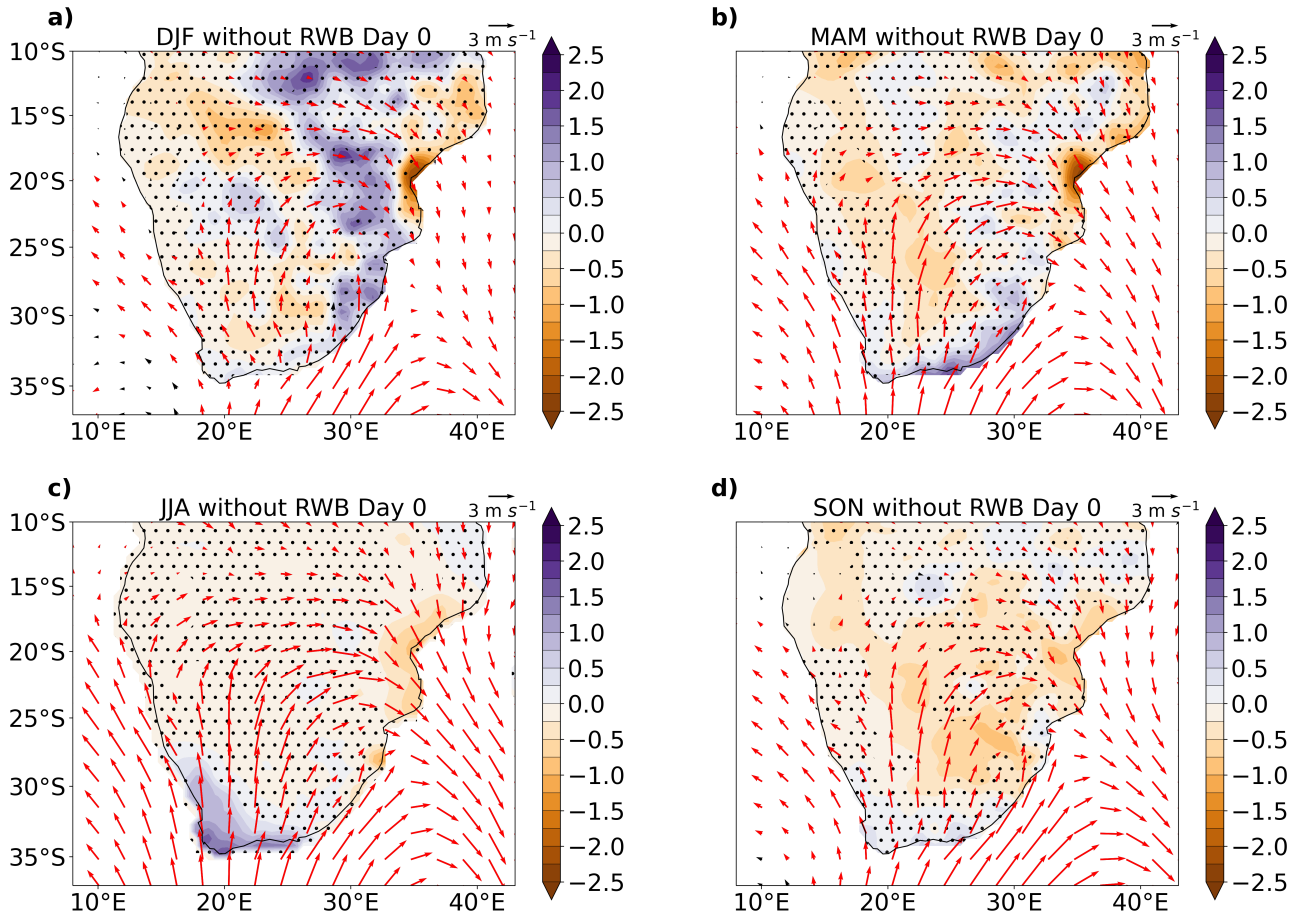

Figure S6. Seasonal composites of day 0 of ridging highs without RWB from observations for the period 1980-2009 for summer (a), autumn (b), winter (c) and spring (d). Seasonal anomalies of precipitation (mm day^{-1}) are depicted by the color shading and seasonal anomalies of the 850 hPa winds (m s^{-1}) are depicted by the vectors. The stippling masks anomalies that are **not** significant at the 95% confidence interval based on the Monte Carlo method. The red vectors depict significant wind anomalies.

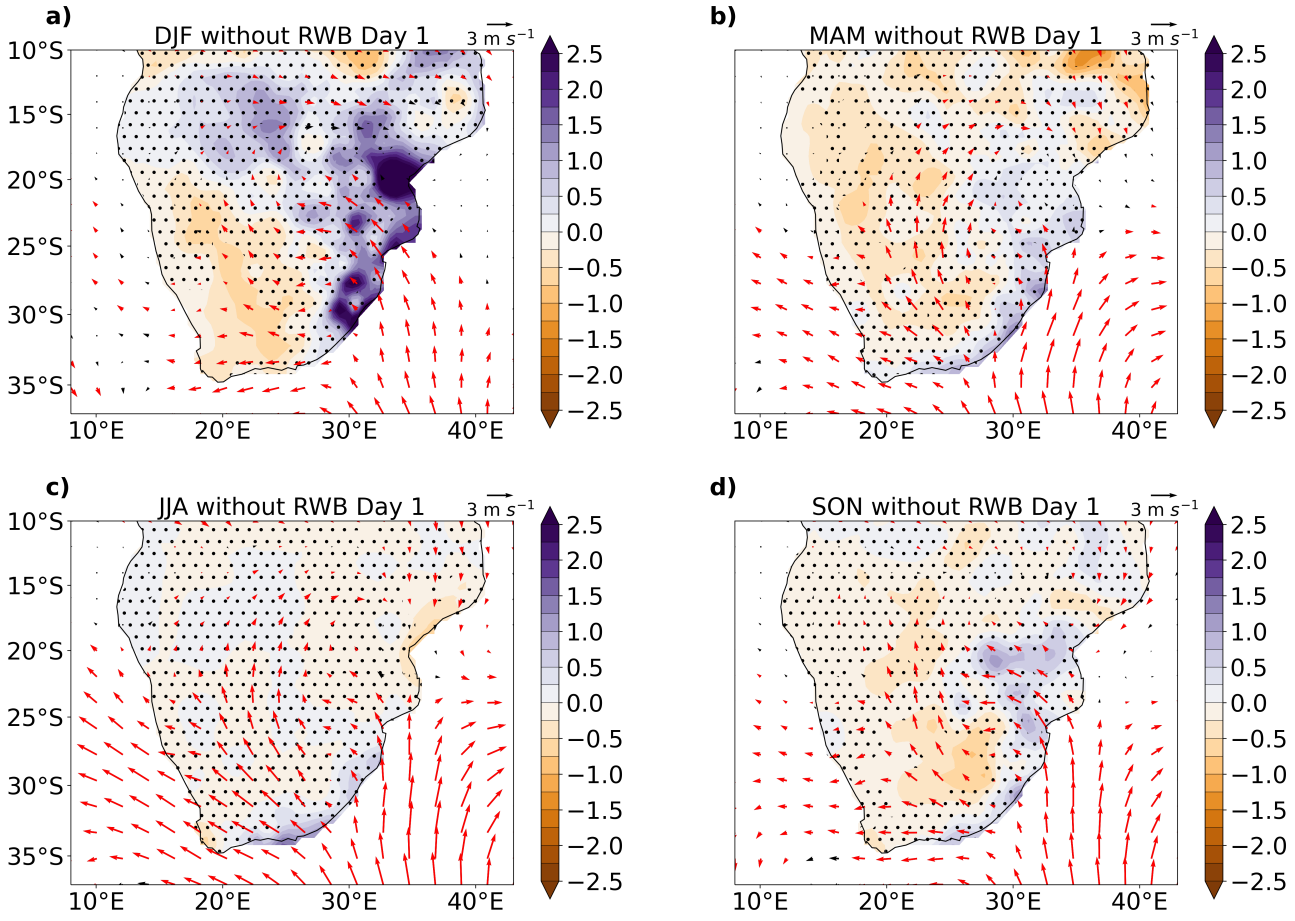

Figure S7. Seasonal composites of day 1 of ridging highs without RWB from observations for the period 1980-2009 for summer (a), autumn (b), winter (c) and spring (d). Seasonal anomalies of precipitation (mm day^{-1}) are depicted by the color shading and seasonal anomalies of the 850 hPa winds (m s^{-1}) are depicted by the vectors. The stippling masks anomalies that are **not** significant at the 95% confidence interval based on the Monte Carlo method. The red vectors depict significant wind anomalies.